STABILIZED FINITE ELEMENTS FOR TRESCA FRICTION PROBLEM

TOM GUSTAFSSON AND JUHA VIDEMAN

Abstract. We formulate and analyze a Nitsche-type algorithm for frictional contact problems. The method is derived from, and analyzed as, a stabilized finite element method and shown to be quasi-optimal, as well as suitable as an adaptive scheme through an a posteriori error analysis. The a posteriori error indicators are validated in a numerical experiment.

1. Introduction

The frictionless contact between deforming bodies can be interpreted as a minimization problem with a nonpeneration constraint imposed on the displacement field, see, *e.g.*, [1, 2, 3]. When the friction between the bodies is taken into account, the contact is usually modelled through a solution-dependent upper bound function for the tangential traction (Coulomb friction model), see, *e.g.*, [4, 1]. If the upper bound function is prescribed, the Coulomb friction model simplifies to the Tresca friction problem.

In both friction models, the constraints can be resolved with the help of Lagrange multipliers. The variational inequalities corresponding to the mixed formulation of these contact problems have a saddle point structure and their approximation by standard finite elements leads to unstable and ill-conditioned methods. In particular, the methods are stable if and only if the chosen finite element spaces satisfy the Babuška–Brezzi inf-sup condition which is nontrivial in the general case of nonmatching meshes. Consequently, special finite element bases have been developed for the Lagrange multiplier that address the stability and lead to optimally convergent methods, see [5] and all the references therein.

As an alternative to a mixed method, we consider a stabilized finite element method. To keep the notation and the presentation simple and readable, we restrict ourselves to the unilateral contact between a deformable body and a rigid foundation and consider the Tresca friction problem. We note, however, that it is straightforward to extend our method to contact between two deformable bodies. Besides avoiding the Babuška–Brezzi inf-sup condition, the stabilized method provides an elegant way to derive and justify the use of Nitsche's method for approximating frictional contact problems, cf. [6, 7, 8]. Most importantly, building upon the stabilized formulation we are able to prove the efficiency and reliability of residual-based a posteriori error estimators for Nitsche's method without extra regularity assumptions or resorting to a saturation assumption as in [8].

In this work, we capitalize on the analysis of stabilized finite element methods for variational inequalities, first presented in [9] and recently extended to frictionless contact problems in [10], see also [11]. We will omit some of the proofs (*e.g.*, the continuous stability estimate) that would follow step by step the reasoning

This provisional PDF is the accepted version. The article should be cited as: ESAIM: M2AN, doi: 10.1051/m2an/2022048

presented in detail in [9, 10] and instead put more emphasis on the a posteriori error indicators in adaptive schemes as well as discuss the practical implementation of the method as a Nitsche-type numerical algorithm. The algorithm is validated in a numerical experiment using open source software and the source code is freely available [12].

The numerical approximation of frictional contact between deformable bodies has a long-lived history, see, *e.g.*, [1, 13, 3, 5] and all the references therein. Different approaches abound, ranging from mixed saddle-point formulations based on dual Lagrange multipliers ([14, 15, 16, 17, 18, 5]) to Nitsche-type method ([6, 8, 19]). For a posteriori error analyses of the frictional contact problem based on the saddle-point formulation, we refer to [20, 21, 5] and based on Nitsche's formulation to the Appendix in [8].

The article is organized as follows. In Section 2, we explain the problem setting, in Section 3 give a variational formulation to the Tresca friction problem, in Section 4 formulate our finite element scheme and in Section 5 show quasi-optimality of the method and perform the a posteriori error analysis. In Section 6, we derive Nitsche's method from the stabilized method, introduce an algorithm for the practical computation of the numerical solution and discuss implementional aspects. Finally, in Section 7 we present a numerical experiment to corroborate the usefulness of the a posteriori error indicators.

2. Tresca friction problem

Let $\Omega \subset \mathbb{R}^d$, $d \in \{2, 3\}$, denote a deformable polygonal (polyhedral) body. The boundary $\partial\Omega$ is split into three parts Γ_D, Γ_N and Γ, with Γ_D denoting the part where the displacement of the body is zero, Γ_N the part of the boundary with zero traction and Γ the part where contact between the body and a rigid foundation can occur. The parts Γ_D and Γ are assumed to be separated by Γ_N, i.e. $\overline{\Gamma_D} \cap \overline{\Gamma} = \varnothing$, and Γ is a straight line if $d = 2$ or a planar polygon if $d = 3$. Assuming that Γ_D and Γ are separated, we avoid introducing the Lions-Magenes space $H_{00}^{1/2}(\Gamma)$.

Let $\boldsymbol{u} : \Omega \to \mathbb{R}^d$, denote the displacement of the body Ω. The infinitesimal strain tensor reads

$$\boldsymbol{\varepsilon}(\boldsymbol{u}) = \frac{1}{2}\Big(\nabla \boldsymbol{u} + (\nabla \boldsymbol{u})^T\Big), \tag{1}$$

and the stress tensor is given by

$$\boldsymbol{\sigma}(\boldsymbol{u}) = 2\mu\, \boldsymbol{\varepsilon}(\boldsymbol{u}) + \lambda \operatorname{tr} \boldsymbol{\varepsilon}(\boldsymbol{u}) \boldsymbol{I}, \tag{2}$$

where μ and λ are the Lamé parameters and $\boldsymbol{I}$ is an identity tensor. We define the normal component of $\boldsymbol{u}$ as $u_n = \boldsymbol{u} \cdot \boldsymbol{n}$ where $\boldsymbol{n} : \partial\Omega \to \mathbb{R}^d$ denotes the outward unit normal to the body Ω. The traction vector $\boldsymbol{\sigma}(\boldsymbol{u})\boldsymbol{n}$ is split into the normal component $\sigma_n(\boldsymbol{u})\boldsymbol{n}$, $\sigma_n(\boldsymbol{u}) = \boldsymbol{\sigma}(\boldsymbol{u})\boldsymbol{n} \cdot \boldsymbol{n}$, and the tangential component $\boldsymbol{\sigma}_t(\boldsymbol{u}) = \boldsymbol{\sigma}(\boldsymbol{u})\boldsymbol{n} - \sigma_n(\boldsymbol{u})\boldsymbol{n}$. Similarly, we define the tangential displacement as $\boldsymbol{u}_t = \boldsymbol{u} - u_n\boldsymbol{n}$.

The governing equation and the boundary conditions read as follows

$$-\mathbf{div}\, \boldsymbol{\sigma}(\boldsymbol{u}) = \boldsymbol{f} \quad \text{in } \Omega, \tag{3}$$

$$\boldsymbol{u} = \boldsymbol{0} \quad \text{on } \Gamma_D, \tag{4}$$

$$\boldsymbol{\sigma}(\boldsymbol{u})\boldsymbol{n} = \boldsymbol{0} \quad \text{on } \Gamma_N, \tag{5}$$

where $\boldsymbol{f} \in [L^2(\Omega)]^d$ is the volumetric force. The physical nonpenetration condition on Γ is

$$u_n - g \leq 0, \quad \sigma_n(\boldsymbol{u}) \leq 0, \quad \sigma_n(\boldsymbol{u})(u_n - g) = 0, \tag{6}$$

where $g \in H^{1/2}(\Gamma)$ is the gap between the body and a rigid foundation in the direction of $\boldsymbol{n}$. The Tresca friction condition on Γ reads as (cf. [4, 1])

$$\begin{cases} |\boldsymbol{\sigma}_t(\boldsymbol{u})| \leq \kappa, \\ |\boldsymbol{\sigma}_t(\boldsymbol{u})| < \kappa \Rightarrow \boldsymbol{u}_t = \boldsymbol{0}, \\ |\boldsymbol{\sigma}_t(\boldsymbol{u})| = \kappa > 0 \Rightarrow \exists \nu \geq 0 : \boldsymbol{u}_t = -\nu \boldsymbol{\sigma}_t(\boldsymbol{u}), \end{cases} \tag{7}$$

where $\kappa \in L^2(\Gamma)$, $\kappa \geq 0$ a.e. in Γ, is a given upper limit for the tangential traction before slip can occur.

The Tresca friction problem can be written as a mixed problem by introducing a dual variable (Lagrange multiplier) $\boldsymbol{\lambda} = -\boldsymbol{\sigma}(\boldsymbol{u})\boldsymbol{n}$, and considering separately its normal and tangential components, $\lambda_n = -\sigma_n(\boldsymbol{u})$ and $\boldsymbol{\lambda}_t = \boldsymbol{\lambda} - \lambda_n \boldsymbol{n}$.

Problem 1 (mixed formulation)**.** *Find* $(\boldsymbol{u}, \boldsymbol{\lambda})$ *satisfying*

$$-\mathbf{div}\, \boldsymbol{\sigma}(\boldsymbol{u}) = \boldsymbol{f} \quad \text{in } \Omega, \tag{8}$$

$$\boldsymbol{u} = \boldsymbol{0} \quad \text{on } \Gamma_D, \tag{9}$$

$$\boldsymbol{\sigma}(\boldsymbol{u})\boldsymbol{n} = \boldsymbol{0} \quad \text{on } \Gamma_N, \tag{10}$$

$$\boldsymbol{\lambda} + \boldsymbol{\sigma}(\boldsymbol{u})\boldsymbol{n} = \boldsymbol{0} \quad \text{on } \Gamma, \tag{11}$$

with the contact conditions

$$\begin{cases} \lambda_n \geq 0, \\ u_n - g \leq 0, \\ \lambda_n(u_n - g) = 0, \end{cases} \quad \text{on } \Gamma, \tag{12}$$

and the friction conditions

$$\begin{cases} |\boldsymbol{\lambda}_t| \leq \kappa, \\ |\boldsymbol{\lambda}_t| < \kappa \Rightarrow \boldsymbol{u}_t = \boldsymbol{0}, \\ |\boldsymbol{\lambda}_t| = \kappa > 0 \Rightarrow \exists \nu \geq 0 : \boldsymbol{u}_t = \nu \boldsymbol{\lambda}_t, \end{cases} \quad \text{on } \Gamma. \tag{13}$$

3. Variational formulation

We will now present a variational formulation for Problem 1. For the primal variable, we consider the standard Sobolev space

$$\boldsymbol{V} = \{\boldsymbol{w} \in [H^1(\Omega)]^d : \boldsymbol{w}|_{\Gamma_D} = \boldsymbol{0}\}. \tag{14}$$

To introduce the spaces for the functions defined on Γ, we use a local orthonormal basis $\{\boldsymbol{n}(\boldsymbol{x}), \boldsymbol{t}(\boldsymbol{x})\}$ for $d = 2$ and $\{\boldsymbol{n}(\boldsymbol{x}), \boldsymbol{t}_1(\boldsymbol{x}), \boldsymbol{t}_2(\boldsymbol{x})\}$ for $d = 3$ at $\boldsymbol{x} \in \Gamma$, and split the trace $\boldsymbol{w}|_\Gamma$ into normal and tangential components, i.e.

$$\boldsymbol{w}(\boldsymbol{x}) = (w_n(\boldsymbol{x}), \boldsymbol{w}_t(\boldsymbol{x})) \in \mathbb{R} \times \mathbb{R}^{d-1}$$

for any $\boldsymbol{x} \in \Gamma$. Consequently, the trace of $\boldsymbol{w} \in \boldsymbol{V}$ on Γ belongs to $H^{1/2}(\Gamma) \times (H^{1/2}(\Gamma))^{d-1}$ with the norm

$$\|(w_n, \boldsymbol{w}_t)\|^2_{\frac{1}{2},\Gamma} = \|w_n\|^2_{\frac{1}{2},\Gamma} + \|\boldsymbol{w}_t\|^2_{\frac{1}{2},\Gamma}$$

where

$$\|w\|_{\frac{1}{2},\Gamma} = \inf_{v\in H^1(\Omega), v|_\Gamma = w} \|v\|_1, \quad \text{and} \quad \|\boldsymbol{w}\|^2_{\frac{1}{2},\Gamma} = \sum_{i=1}^{d-1} \|w_i\|^2_{\frac{1}{2},\Gamma}.$$

This splitting allows treating separately the normal and the tangential components of the Lagrange multiplier vector which in the Tresca friction formulation are uncoupled. To this end, we define the spaces

$$\begin{aligned}
\Lambda_n &= \{\mu \in H^{-1/2}(\Gamma) : \langle v, \mu\rangle \geq 0 \ \forall v \in H^{1/2}(\Gamma), v \geq 0 \text{ a.e. in } \Gamma\},\\
\boldsymbol{\Lambda}_t &= \{\boldsymbol{\mu} \in (H^{-1/2}(\Gamma))^{d-1} : \langle \boldsymbol{v}, \boldsymbol{\mu}\rangle \leq (\kappa, |\boldsymbol{v}|)_\Gamma \ \forall \boldsymbol{v} \in (H^{1/2}(\Gamma))^{d-1}\},
\end{aligned}$$

where by $\langle\cdot,\cdot\rangle : H^{1/2}(\Gamma) \times H^{-1/2}(\Gamma) \to \mathbb{R}$ we denote the duality pairing and, for $(\boldsymbol{w}, \boldsymbol{\xi}) \in (H^{1/2}(\Gamma))^{d-1} \times (H^{-1/2}(\Gamma))^{d-1}$, write $\langle \boldsymbol{w}, \boldsymbol{\xi}\rangle = \sum_{i=1}^{d-1} \langle w_i, \xi_i\rangle$. The dual space $H^{-1/2}(\Gamma)$ and the vectorial dual space $(H^{-1/2}(\Gamma))^{d-1}$ are equipped with the norms

$$\|\xi\|_{-\frac{1}{2},\Gamma} = \sup_{v\in H^{1/2}(\Gamma)} \frac{\langle v, \xi\rangle}{\|v\|_{\frac{1}{2},\Gamma}} \quad \text{and} \quad \|\boldsymbol{\xi}\|^2_{-\frac{1}{2},\Gamma} = \sum_{i=1}^{d-1} \|\xi_i\|^2_{-\frac{1}{2},\Gamma},$$

respectively. Moreover, we let $\boldsymbol{Q} = H^{-1/2}(\Gamma) \times (H^{-1/2}(\Gamma))^{d-1}$ and define a bilinear form $\mathcal{B} : (\boldsymbol{V} \times \boldsymbol{Q}) \times (\boldsymbol{V} \times \boldsymbol{Q}) \to \mathbb{R}$ through

$$\mathcal{B}(\boldsymbol{w}, \boldsymbol{\xi}; \boldsymbol{v}, \boldsymbol{\mu}) = (\boldsymbol{\sigma}(\boldsymbol{w}), \boldsymbol{\varepsilon}(\boldsymbol{v}))_\Omega + b(\boldsymbol{v}, \boldsymbol{\xi}) + b(\boldsymbol{w}, \boldsymbol{\mu}), \tag{15}$$

where $b(\boldsymbol{w}, \boldsymbol{\xi}) = \langle w_n, \xi_n\rangle + \langle \boldsymbol{w}_t, \boldsymbol{\xi}_t\rangle$ for any $\boldsymbol{w} \in \boldsymbol{V}$ and $\boldsymbol{\xi} = (\xi_n, \boldsymbol{\xi}_t) \in \boldsymbol{Q}$. We also define a linear form $\mathcal{L} : \boldsymbol{V} \times \boldsymbol{Q} \to \mathbb{R}$ by

$$\mathcal{L}(\boldsymbol{v}, \boldsymbol{\mu}) = (\boldsymbol{f}, \boldsymbol{v})_\Omega + \langle g, \mu_n\rangle. \tag{16}$$

Let $\boldsymbol{\Lambda} = \Lambda_n \times \boldsymbol{\Lambda}_t \subset \boldsymbol{Q}$. It is now straightforward to write Problem 1 as the following variational inequality.

Problem 2 (variational formulation)**.** *Find* $(\boldsymbol{u}, \boldsymbol{\lambda}) \in \boldsymbol{V} \times \boldsymbol{\Lambda}$ *such that*

$$\mathcal{B}(\boldsymbol{u}, \boldsymbol{\lambda}; \boldsymbol{v}, \boldsymbol{\mu} - \boldsymbol{\lambda}) \leq \mathcal{L}(\boldsymbol{v}, \boldsymbol{\mu} - \boldsymbol{\lambda}) \quad \forall (\boldsymbol{v}, \boldsymbol{\mu}) \in \boldsymbol{V} \times \boldsymbol{\Lambda}.$$

Remark 1. The corresponding primal variational formulation of the Tresca friction problem reads as follows: find $\boldsymbol{u} \in \boldsymbol{K} = \{\boldsymbol{v} \in \boldsymbol{V} : v_n - g \leq 0 \text{ a.e. on } \Gamma\}$ such that

$$(\boldsymbol{\sigma}(\boldsymbol{u}), \boldsymbol{\varepsilon}(\boldsymbol{v} - \boldsymbol{u}))_\Omega + (\kappa, |\boldsymbol{v}_t|)_\Gamma - (\kappa, |\boldsymbol{u}_t|)_\Gamma \leq (\boldsymbol{f}, \boldsymbol{v} - \boldsymbol{u})_\Omega \quad \forall \boldsymbol{v} \in \boldsymbol{K}.$$

The existence of a unique solution to this variational inequality of the second kind is classical, cf. [4, 1, 2]. However, the nondifferentiable term $(\kappa, |\boldsymbol{v}_t|)_\Gamma$ makes the primal formulation less amenable to numerical approximation than the mixed formulation. The equivalence between the mixed and the primal formulations has been established in [14], see also [15, 16].

Remark 2. Since $\kappa \in L^2(\Gamma)$ and the contact region is smooth, the tangential traction is in fact a $L^2(\Gamma)$-function, cf. [22], and the set $\boldsymbol{\Lambda}_t$ is often defined using this extra regularity, cf. [2, 15, 16]. The error estimates for $\boldsymbol{\lambda}_t$ are, however, naturally obtained in the $H^{-1/2}(\Gamma)$-norm and the definition chosen here for $\boldsymbol{\Lambda}_t$ can be naturally extended to the Coulomb friction case, cf. [5]. Moreover, the stabilization terms defined below are related with discrete $H^{-1/2}(\Gamma)$-norms and the resulting stabilized method leads to the Nitsche's method presented in the literature [6, 23, 7].

The variational formulation will be analyzed in the norm

$$\|(\boldsymbol{w},\boldsymbol{\xi})\|^2 = |||\boldsymbol{w}|||^2 + \|\xi_n\|^2_{-\frac{1}{2},\Gamma} + \|\boldsymbol{\xi}_t\|^2_{-\frac{1}{2},\Gamma} \tag{17}$$

where

$$|||\boldsymbol{w}|||^2 = (\boldsymbol{\sigma}(\boldsymbol{w}),\boldsymbol{\varepsilon}(\boldsymbol{w}))_\Omega. \tag{18}$$

The proof of the following result is quite standard, see, *e.g.*, [10], for more details.

Theorem 1 (continuous stability)**.** *For every* $(\boldsymbol{w},\boldsymbol{\xi}) \in \boldsymbol{V}\times\boldsymbol{Q}$ *there exists* $\boldsymbol{v}\in\boldsymbol{V}$ *and constants* $C_1, C_2 > 0$ *such that*

$$\mathcal{B}(\boldsymbol{w},\boldsymbol{\xi};\boldsymbol{v},-\boldsymbol{\xi}) \geq C_1\|(\boldsymbol{w},\boldsymbol{\xi})\|^2 \tag{19}$$

and

$$|||\boldsymbol{v}||| \leq C_2\|(\boldsymbol{w},\boldsymbol{\xi})\|. \tag{20}$$

4. Finite element method

Let $\mathcal{T}_h$ denote a subdivision of the domain Ω into nonoverlapping elements, triangles ($d=2$) or tetrahedra ($d=3$), with h denoting the global mesh parameter. We denote by $\mathcal{G}_h$ the trace mesh of $\mathcal{T}_h$ on Γ, consisting of edge segments ($d=2$) or facet triangles ($d=3$) of the elements in $\mathcal{T}_h$. The set of interior edges/facets are denoted by $\mathcal{E}_h$ and the set of boundary edges/facets belonging to the boundary Γ_N by $\mathcal{F}_h$. In what follows, we write $a \lesssim b$ if $a \leq Cb$ for some $C>0$ independent of the mesh parameter h; similarly for $a \gtrsim b$.

Aiming at constructing a uniformly stable approximation of Problem 2, we augment the bilinear form $\mathcal{B}$ using the residual of (11) as follows:

$$\mathcal{B}_h(\boldsymbol{w},\boldsymbol{\xi};\boldsymbol{v},\boldsymbol{\mu}) = \mathcal{B}(\boldsymbol{w},\boldsymbol{\xi};\boldsymbol{v},\boldsymbol{\mu}) - \alpha\sum_{E\in\mathcal{G}_h} h_E(\boldsymbol{\xi}+\boldsymbol{\sigma}(\boldsymbol{w})\boldsymbol{n},\boldsymbol{\mu}+\boldsymbol{\sigma}(\boldsymbol{v})\boldsymbol{n})_E \tag{21}$$

where $\alpha > 0$ is a stabilization parameter and h_E is the local mesh parameter corresponding to $E\in\mathcal{G}_h$. The finite element spaces $\boldsymbol{V}_h \subset \boldsymbol{V}$ and $\boldsymbol{Q}_h \subset \boldsymbol{Q}$ are defined as

$$\boldsymbol{V}_h = \{\boldsymbol{w}\in\boldsymbol{V} : \boldsymbol{w}|_K \in [P_m(K)]^d \ \forall K\in\mathcal{T}_h\}, \tag{22}$$

$$\boldsymbol{Q}_h = \{(\mu_n,\boldsymbol{\mu}_t)\in\boldsymbol{Q} : \mu_n|_E \in P_l(E) \text{ and } \boldsymbol{\mu}_t|_E \in [P_l(E)]^{d-1} \ \forall E\in\mathcal{G}_h\}, \tag{23}$$

where $m\geq 1$ and $l\geq 0$ denote the polynomial orders. In addition, we define the convex subset

$$\boldsymbol{\Lambda}_h = \{(\mu_n,\boldsymbol{\mu}_t)\in\boldsymbol{Q}_h : \mu_n \geq 0,\ |\boldsymbol{\mu}_t| \leq \kappa\} \subset \boldsymbol{\Lambda}. \tag{24}$$

The stabilized finite element method corresponds to solving the following variational problem.

Problem 3 (discrete formulation)**.** *Find* $(\boldsymbol{u}_h,\boldsymbol{\lambda}_h)\in\boldsymbol{V}_h\times\boldsymbol{\Lambda}_h$ *such that*

$$\mathcal{B}_h(\boldsymbol{u}_h,\boldsymbol{\lambda}_h;\boldsymbol{v}_h,\boldsymbol{\mu}_h-\boldsymbol{\lambda}_h) \leq \mathcal{L}(\boldsymbol{v}_h,\boldsymbol{\mu}_h-\boldsymbol{\lambda}_h) \quad \forall(\boldsymbol{v}_h,\boldsymbol{\mu}_h)\in\boldsymbol{V}_h\times\boldsymbol{\Lambda}_h. \tag{25}$$

We will show in Theorem 2 below that the discrete formulation is stable in the following mesh-dependent norm:

$$\|(\boldsymbol{v},\boldsymbol{\mu})\|_h^2 = \|(\boldsymbol{v},\boldsymbol{\mu})\|^2 + \sum_{E\in\mathcal{G}_h} h_E\|\boldsymbol{\mu}\|^2_{0,E}, \quad (\boldsymbol{v},\boldsymbol{\mu})\in\boldsymbol{V}_h\times\boldsymbol{Q}_h. \tag{26}$$

In the proof, we will use the following discrete trace estimate, established using a scaling argument.

Lemma 1. *For any $\boldsymbol{w}_h \in \boldsymbol{V}_h$, there exists $C_I > 0$ such that*

$$C_I \sum_{E \in \mathcal{G}_h} h_E \|\boldsymbol{\sigma}(\boldsymbol{w}_h)\boldsymbol{n}\|_{0,E}^2 \leq |||\boldsymbol{w}_h|||^2. \tag{27}$$

The existence and uniqueness of the discrete problem is a consequence of the following stability estimate:

Theorem 2 (discrete stability)**.** *Suppose that $0 < \alpha < C_I$. Then for every $(\boldsymbol{w}_h, \boldsymbol{\xi}_h) \in \boldsymbol{V}_h \times \boldsymbol{Q}_h$ there exists $\boldsymbol{v}_h \in \boldsymbol{V}_h$ satisfying*

$$\mathcal{B}_h(\boldsymbol{w}_h, \boldsymbol{\xi}_h; \boldsymbol{v}_h, -\boldsymbol{\xi}_h) \geq C_1 \|(\boldsymbol{w}_h, \boldsymbol{\xi}_h)\|_h^2 \tag{28}$$

and

$$|||\boldsymbol{v}_h||| \leq C_2 \|(\boldsymbol{w}_h, \boldsymbol{\xi}_h)\|_h. \tag{29}$$

Proof. Using Lemma 1, we first obtain

$$\begin{aligned}\mathcal{B}_h(\boldsymbol{w}_h, \boldsymbol{\xi}_h; \boldsymbol{w}_h, -\boldsymbol{\xi}_h) &= |||\boldsymbol{w}_h|||^2 - \alpha \sum_{E \in \mathcal{G}_h} h_E \|\boldsymbol{\sigma}(\boldsymbol{w}_h)\boldsymbol{n}\|_{0,E}^2 + \alpha \sum_{E \in \mathcal{G}_h} h_E \|\boldsymbol{\xi}_h\|_{0,E}^2 \\ &\geq \left(1 - \frac{\alpha}{C_I}\right) |||\boldsymbol{w}_h|||^2 + \alpha \sum_{E \in \mathcal{G}_h} h_E \|\boldsymbol{\xi}_h\|_{0,E}^2.\end{aligned}$$

On the other hand, the continuous stability estimate implies that there exists $\boldsymbol{v} \in \boldsymbol{V}$ such that for any $\boldsymbol{\xi}_h \in \boldsymbol{Q}_h$ it holds

$$b(\boldsymbol{v}, \boldsymbol{\xi}_h) \geq C_1 (\|\xi_{h,n}\|_{-\frac{1}{2},\Gamma}^2 + \|\boldsymbol{\xi}_{h,t}\|_{-\frac{1}{2},\Gamma}^2) \tag{30}$$

and, moreover,

$$|||\boldsymbol{v}|||^2 \leq C_2 (\|\xi_{h,n}\|_{-\frac{1}{2},\Gamma}^2 + \|\boldsymbol{\xi}_{h,t}\|_{-\frac{1}{2},\Gamma}^2). \tag{31}$$

Let $\widetilde{\boldsymbol{v}} \in \boldsymbol{V}_h$ now be the Clément interpolant of $\boldsymbol{v}$. It follows that

$$\begin{aligned} b(\widetilde{\boldsymbol{v}}, \boldsymbol{\xi}_h) &= b(\widetilde{\boldsymbol{v}} - \boldsymbol{v}, \boldsymbol{\xi}_h) + b(\boldsymbol{v}, \boldsymbol{\xi}_h) \\ &\geq - \sum_{E \in \mathcal{G}_h} h_E^{-1/2} \|v_n - \widetilde{v}_n\|_{0,E} \, h_E^{1/2} \|\xi_{h,n}\|_{0,E} \\ &\quad - \sum_{E \in \mathcal{G}_h} h_E^{-1/2} \|\boldsymbol{v}_t - \widetilde{\boldsymbol{v}}_t\|_{0,E} \, h_E^{1/2} \|\boldsymbol{\xi}_{h,t}\|_{0,E} \\ &\quad + C_1 (\|\xi_{h,n}\|_{-\frac{1}{2},\Gamma}^2 + \|\boldsymbol{\xi}_{h,t}\|_{-\frac{1}{2},\Gamma}^2) \\ &\geq - \left(\sum_{E \in \mathcal{G}_h} h_E^{-1} \|v_n - \widetilde{v}_n\|_{0,E}^2 \right)^{1/2} \left(\sum_{E \in \mathcal{G}_h} h_E \|\xi_{h,n}\|_{0,E}^2 \right)^{1/2} \\ &\quad - \left(\sum_{E \in \mathcal{G}_h} h_E^{-1} \|\boldsymbol{v}_t - \widetilde{\boldsymbol{v}}_t\|_{0,E}^2 \right)^{1/2} \left(\sum_{E \in \mathcal{G}_h} h_E \|\boldsymbol{\xi}_{h,t}\|_{0,E}^2 \right)^{1/2} \\ &\quad + C_1 (\|\xi_{h,n}\|_{-\frac{1}{2},\Gamma}^2 + \|\boldsymbol{\xi}_{h,t}\|_{-\frac{1}{2},\Gamma}^2) \\ &\geq -C_3 |||\boldsymbol{v}||| \left(\sum_{E \in \mathcal{G}_h} h_E \|\boldsymbol{\xi}_h\|_{0,E}^2 \right)^{1/2} + C_1 (\|\xi_{h,n}\|_{-\frac{1}{2},\Gamma}^2 + \|\boldsymbol{\xi}_{h,t}\|_{-\frac{1}{2},\Gamma}^2) \\ &\geq -C_4 \sum_{E \in \mathcal{G}_h} h_E \|\boldsymbol{\xi}_h\|_{0,E}^2 + C_5 (\|\xi_{h,n}\|_{-\frac{1}{2},\Gamma}^2 + \|\boldsymbol{\xi}_{h,t}\|_{-\frac{1}{2},\Gamma}^2). \end{aligned} \tag{32}$$

where we have used Young's inequality, estimates (30) and (31), and the following properties of the Clément interpolant:

$$\sum_{E\in\mathcal{G}_h} h_E^{-1}\|\boldsymbol{v}-\widetilde{\boldsymbol{v}}\|_{0,E}^2 \lesssim |||\boldsymbol{v}|||^2 \quad \text{and} \quad |||\widetilde{\boldsymbol{v}}||| \lesssim |||\boldsymbol{v}|||. \tag{33}$$

Finally, combining the estimates above, we obtain the bound

$$\begin{aligned}
&\mathcal{B}_h(\boldsymbol{w}_h,\boldsymbol{\xi}_h;\boldsymbol{w}_h+\delta\widetilde{\boldsymbol{v}},-\boldsymbol{\xi}_h)\\
&\geq \left(1-\frac{\alpha}{C_I}\right)|||\boldsymbol{w}_h|||^2+\alpha\sum_{E\in\mathcal{G}_h} h_E\|\boldsymbol{\xi}_h\|_{0,E}^2\\
&\quad -\delta|||\boldsymbol{w}_h|||\,|||\widetilde{\boldsymbol{v}}||| + \delta b(\widetilde{\boldsymbol{v}},\boldsymbol{\xi}_h) - \alpha\delta\sum_{E\in\mathcal{G}_h} h_E(\boldsymbol{\xi}_h+\boldsymbol{\sigma}(\boldsymbol{w}_h)\boldsymbol{n},\boldsymbol{\sigma}(\widetilde{\boldsymbol{v}})\boldsymbol{n})_E\\
&\gtrsim \|(\boldsymbol{w}_h,\boldsymbol{\xi}_h)\|_h^2,
\end{aligned}$$

where the last step follows, choosing $\delta>0$ small enough, from Young's inequality, estimates (31), (32) and (33), and Lemma 1. □

5. Error analysis

Let $\boldsymbol{f}_h\in\boldsymbol{V}_h$ be the $[L^2(\Omega)]^d$-projection of $\boldsymbol{f}$. For any $K\in\mathcal{T}_h$, we define the oscillation of $\boldsymbol{f}$ by $\mathrm{osc}_K(\boldsymbol{f})=h_K\|\boldsymbol{f}-\boldsymbol{f}_h\|_{0,K}$. Moreover, we denote by $K(E)\in\mathcal{T}_h$ the element having $E\in\mathcal{G}_h$ as one of its facets, i.e., $\partial K(E)\cap E=E$.

Lemma 2. *For any $(\boldsymbol{w}_h,\boldsymbol{\xi}_h)\in\boldsymbol{V}_h\times\boldsymbol{\Lambda}_h$ it holds that*

$$\begin{aligned}
&\left(\sum_{E\in\mathcal{G}_h} h_E\|\boldsymbol{\xi}_h+\boldsymbol{\sigma}(\boldsymbol{w}_h)\boldsymbol{n}\|_{0,E}^2\right)^{1/2}\\
&\qquad\lesssim \|(\boldsymbol{u}-\boldsymbol{w}_h,\boldsymbol{\lambda}-\boldsymbol{\xi}_h)\| + \left(\sum_{E\in\mathcal{G}_h}\mathrm{osc}_{K(E)}(\boldsymbol{f})^2\right)^{1/2}.
\end{aligned}$$

Proof. Let $b_E:E\to[0,1]$, $b_E\in P_d(E)$, denote the facet bubble with $b_E=1$ in the middle of E and $b_E=0$ on the boundary ∂E. Then we have

$$h_E\|\boldsymbol{\xi}_h+\boldsymbol{\sigma}(\boldsymbol{w}_h)\boldsymbol{n}\|_{0,E}^2 \lesssim (\boldsymbol{\xi}_h+\boldsymbol{\sigma}(\boldsymbol{w}_h)\boldsymbol{n},\boldsymbol{\tau}_E)_E \tag{34}$$

where

$$\boldsymbol{\tau}_E|_E = b_E h_E(\boldsymbol{\xi}_h+\boldsymbol{\sigma}(\boldsymbol{w}_h)\boldsymbol{n}) \quad \text{and} \quad \boldsymbol{\tau}_E|_{\partial K(E)\setminus E}=\boldsymbol{0}.$$

Choosing $\boldsymbol{v}=\boldsymbol{\tau}$ in Problem 2 with $\boldsymbol{\tau}=\sum_{E\in\mathcal{G}_h}\boldsymbol{\tau}_E$ gives

$$0=-(\boldsymbol{\sigma}(\boldsymbol{u}),\boldsymbol{\varepsilon}(\boldsymbol{\tau}))-b(\boldsymbol{\tau},\boldsymbol{\lambda})+(\boldsymbol{f},\boldsymbol{\tau}).$$

Summing (34) over the edges $E\in\mathcal{G}_h$ and using the above equality gives

$$\begin{aligned}
&\sum_{E\in\mathcal{G}_h} h_E\|\boldsymbol{\xi}_h+\boldsymbol{\sigma}(\boldsymbol{w}_h)\boldsymbol{n}\|_{0,E}^2\\
&\lesssim (\boldsymbol{\xi}_h+\boldsymbol{\sigma}(\boldsymbol{w}_h)\boldsymbol{n},\boldsymbol{\tau})_\Gamma\\
&= (\boldsymbol{\xi}_h,\boldsymbol{\tau})_\Gamma+(\boldsymbol{\sigma}(\boldsymbol{w}_h)\boldsymbol{n},\boldsymbol{\tau})_\Gamma-(\boldsymbol{\sigma}(\boldsymbol{u}),\boldsymbol{\varepsilon}(\boldsymbol{\tau}))-b(\boldsymbol{\tau},\boldsymbol{\lambda})+(\boldsymbol{f},\boldsymbol{\tau})\\
&= b(\boldsymbol{\tau},\boldsymbol{\xi}_h-\boldsymbol{\lambda})+(\boldsymbol{\sigma}(\boldsymbol{w}_h)\boldsymbol{n},\boldsymbol{\tau})_\Gamma-(\boldsymbol{\sigma}(\boldsymbol{u}),\boldsymbol{\varepsilon}(\boldsymbol{\tau}))+(\boldsymbol{f},\boldsymbol{\tau})\\
&= b(\boldsymbol{\tau},\boldsymbol{\xi}_h-\boldsymbol{\lambda})+(\boldsymbol{\sigma}(\boldsymbol{w}_h-\boldsymbol{u}),\boldsymbol{\varepsilon}(\boldsymbol{\tau}))+(\mathbf{div}\,\boldsymbol{\sigma}(\boldsymbol{w}_h)+\boldsymbol{f},\boldsymbol{\tau}).
\end{aligned}$$

We conclude the proof by estimating the terms on the right-hand side using the Cauchy–Schwarz and trace inequalities, the inverse estimate

$$\|\boldsymbol{\tau}\|_1^2 \lesssim \sum_{E\in\mathcal{G}_h} h_E^{-2}\|\boldsymbol{\tau}_E\|_{0,E}^2,$$

and the standard estimates for interior residuals [24] which give rise to the oscillation term. □

Based on Lemma 2, we will now prove the quasi-optimality of the method. We are deliberately not touching the subject of a priori bounds since we wish to avoid making assumptions on the regularity of the solution (see also Remark 4.1 in [10]).

Theorem 3 (quasi-optimality)**.** *Suppose that* $0 < \alpha < C_I$*. For any* $(\boldsymbol{w}_h, \boldsymbol{\xi}_h) \in \boldsymbol{V}_h \times \boldsymbol{\Lambda}_h$ *it holds*

$$\begin{aligned}\|(\boldsymbol{u}-\boldsymbol{u}_h, \boldsymbol{\lambda}-\boldsymbol{\lambda}_h)\| \lesssim \|(\boldsymbol{u}-\boldsymbol{w}_h, \boldsymbol{\lambda}-\boldsymbol{\xi}_h)\| + \sqrt{(u_n - g, \xi_{h,n})_\Gamma} \\ + \sqrt{\langle \boldsymbol{u}_t, \boldsymbol{\lambda}_t - \boldsymbol{\xi}_{h,t}\rangle} + \left(\sum_{E\in\mathcal{G}_h} \operatorname{osc}_{K(E)}(\boldsymbol{f})^2\right)^{1/2}.\end{aligned}$$

Proof. Let $\boldsymbol{v}_h \in \boldsymbol{V}_h$ be, according to Theorem 2, such that

$$|||\boldsymbol{v}_h||| \lesssim \|(\boldsymbol{u}_h - \boldsymbol{w}_h, \boldsymbol{\lambda}_h - \boldsymbol{\xi}_h)\|_h. \tag{35}$$

From the discrete problem (25) it follows that

$$\mathcal{B}_h(\boldsymbol{u}_h, \boldsymbol{\lambda}_h; \boldsymbol{v}_h, \boldsymbol{\xi}_h - \boldsymbol{\lambda}_h) \le \mathcal{L}(\boldsymbol{v}_h, \boldsymbol{\xi}_h - \boldsymbol{\lambda}_h) \quad \forall \boldsymbol{\xi}_h \in \boldsymbol{\Lambda}_h,$$

and, consequently,

$$\begin{aligned}&\|(\boldsymbol{u}_h - \boldsymbol{w}_h, \boldsymbol{\lambda}_h - \boldsymbol{\xi}_h)\|_h^2 \\ &\lesssim \mathcal{B}_h(\boldsymbol{u}_h - \boldsymbol{w}_h, \boldsymbol{\lambda}_h - \boldsymbol{\xi}_h; \boldsymbol{v}_h, \boldsymbol{\xi}_h - \boldsymbol{\lambda}_h) \\ &\le \mathcal{L}(\boldsymbol{v}_h, \boldsymbol{\xi}_h - \boldsymbol{\lambda}_h) - \mathcal{B}_h(\boldsymbol{w}_h, \boldsymbol{\xi}_h; \boldsymbol{v}_h, \boldsymbol{\xi}_h - \boldsymbol{\lambda}_h) \\ &= \mathcal{L}(\boldsymbol{v}_h, \boldsymbol{\xi}_h - \boldsymbol{\lambda}_h) + \mathcal{B}(\boldsymbol{u} - \boldsymbol{w}_h, \boldsymbol{\lambda} - \boldsymbol{\xi}_h; \boldsymbol{v}_h, \boldsymbol{\xi}_h - \boldsymbol{\lambda}_h) \\ &\quad - \mathcal{B}(\boldsymbol{u}, \boldsymbol{\lambda}; \boldsymbol{v}_h, \boldsymbol{\xi}_h - \boldsymbol{\lambda}_h) + \alpha \sum_{E\in\mathcal{G}_h} h_E(\boldsymbol{\xi}_h + \boldsymbol{\sigma}(\boldsymbol{w}_h)\boldsymbol{n}, \boldsymbol{\xi}_h - \boldsymbol{\lambda}_h + \boldsymbol{\sigma}(\boldsymbol{v}_h)\boldsymbol{n})_E.\end{aligned}$$

The second term above is bounded using the continuity of $\mathcal{B}$. The first and the third terms are simplified using the continuous problem as follows:

$$\begin{aligned}&\mathcal{L}(\boldsymbol{v}_h, \boldsymbol{\xi}_h - \boldsymbol{\lambda}_h) - \mathcal{B}(\boldsymbol{u}, \boldsymbol{\lambda}; \boldsymbol{v}_h, \boldsymbol{\xi}_h - \boldsymbol{\lambda}_h) \\ &= (\boldsymbol{f}, \boldsymbol{v}_h) - (\boldsymbol{\sigma}(\boldsymbol{u}), \boldsymbol{\varepsilon}(\boldsymbol{v}_h)) - b(\boldsymbol{v}_h, \boldsymbol{\lambda}) + \langle g, \xi_{h,n} - \lambda_{h,n}\rangle - b(\boldsymbol{u}, \boldsymbol{\xi}_h - \boldsymbol{\lambda}_h) \\ &= \langle g, \xi_{h,n} - \lambda_{h,n}\rangle - b(\boldsymbol{u}, \boldsymbol{\xi}_h - \boldsymbol{\lambda}_h) \\ &= (g - u_n, \xi_{h,n} - \lambda_{h,n})_\Gamma + \langle \boldsymbol{u}_t, \boldsymbol{\lambda}_{h,t} - \boldsymbol{\xi}_{h,t}\rangle \\ &\le (g - u_n, \xi_{h,n})_\Gamma + (\boldsymbol{u}_t, \boldsymbol{\lambda}_t - \boldsymbol{\xi}_{h,t})_\Gamma,\end{aligned}$$

where the last inequality follows from the fact that we consider a conforming approximation, i.e. $\lambda_{h,n} \ge 0$ and

$$\langle \boldsymbol{u}_t, \boldsymbol{\lambda}_{h,t} - \boldsymbol{\xi}_{h,t}\rangle = \langle \boldsymbol{u}_t, \boldsymbol{\lambda}_t - \boldsymbol{\xi}_{h,t}\rangle + \langle \boldsymbol{u}_t, \boldsymbol{\lambda}_{h,t} - \boldsymbol{\lambda}_t\rangle \le \langle \boldsymbol{u}_t, \boldsymbol{\lambda}_t - \boldsymbol{\xi}_{h,t}\rangle.$$

Finally, we bound the terms due to stabilization as follows:

$$
\begin{aligned}
&\sum_{E\in\mathcal{G}_h} h_E(\boldsymbol{\xi}_h+\boldsymbol{\sigma}(\boldsymbol{w}_h)\boldsymbol{n},\boldsymbol{\xi}_h-\boldsymbol{\lambda}_h+\boldsymbol{\sigma}(\boldsymbol{v}_h)\boldsymbol{n})_E\\
&\lesssim \left(\sum_{E\in\mathcal{G}_h} h_E\|\boldsymbol{\xi}_h+\boldsymbol{\sigma}(\boldsymbol{w}_h)\boldsymbol{n}\|_{0,E}^2\right)^{1/2}\left(\sum_{E\in\mathcal{G}_h} h_E\|\boldsymbol{\xi}_h-\boldsymbol{\lambda}_h+\boldsymbol{\sigma}(\boldsymbol{v}_h)\boldsymbol{n}\|_{0,E}^2\right)^{1/2}\\
&\lesssim \left(\sum_{E\in\mathcal{G}_h} h_E\|\boldsymbol{\xi}_h+\boldsymbol{\sigma}(\boldsymbol{w}_h)\boldsymbol{n}\|_{0,E}^2\right)^{1/2}\\
&\qquad\cdot\left(\sum_{E\in\mathcal{G}_h} h_E\|\boldsymbol{\xi}_h-\boldsymbol{\lambda}_h\|_{0,E}^2+\sum_{E\in\mathcal{G}_h} h_E\|\boldsymbol{\sigma}(\boldsymbol{v}_h)\boldsymbol{n}\|_{0,E}^2\right)^{1/2}\\
&\lesssim \left(\sum_{E\in\mathcal{G}_h} h_E\|\boldsymbol{\xi}_h+\boldsymbol{\sigma}(\boldsymbol{w}_h)\boldsymbol{n}\|_{0,E}^2\right)^{1/2}\|(\boldsymbol{u}_h-\boldsymbol{w}_h,\boldsymbol{\lambda}_h-\boldsymbol{\xi}_h)\|_h
\end{aligned}
$$

where we have used the Cauchy–Schwarz and the triangle inequalities, estimate (35) and Lemma 1. Now, the result follows taking into account Lemma 2 and the trivial bound

$$\|(\boldsymbol{u}_h-\boldsymbol{w}_h,\boldsymbol{\lambda}_h-\boldsymbol{\xi}_h)\|\le\|(\boldsymbol{u}_h-\boldsymbol{w}_h,\boldsymbol{\lambda}_h-\boldsymbol{\xi}_h)\|_h,$$

and using the triangle inequality. □

Remark 3. As mentioned in the introduction, the method we are advocating here, and which we will use in the numerical computations, is a Nitsche-type formulation of the stabilized method, see Section 6. However, the stabilized formulation is more amenable to the error analysis. We also wish to point out that our Nitsche's formulation corresponds essentially to the symmetric version (with $\theta=1$) of the method presented in [6] and that an a priori error analysis was also performed in [6].

Next we define the total error indicator

$$\eta^2=\sum_{K\in\mathcal{T}_h}\eta_K^2+\sum_{E\in\mathcal{E}_h}\eta_{E,\Omega}^2+\sum_{E\in\mathcal{F}_h}\eta_{E,\Gamma_N}^2+\sum_{E\in\mathcal{G}_h}\eta_{E,\Gamma}^2 \tag{36}$$

where the local indicators are given by

$$
\begin{aligned}
\eta_K^2&=h_K^2\|\mathbf{div}\,\boldsymbol{\sigma}(\boldsymbol{u}_h)+\boldsymbol{f}\|_{0,K}^2, && K\in\mathcal{T}_h,\\
\eta_{E,\Omega}^2&=h_E\|[\![\boldsymbol{\sigma}(\boldsymbol{u}_h)\boldsymbol{n}]\!]\|_{0,E}^2, && E\in\mathcal{E}_h,\\
\eta_{E,\Gamma_N}^2&=h_E\|\boldsymbol{\sigma}(\boldsymbol{u}_h)\boldsymbol{n}\|_{0,E}^2, && E\in\mathcal{F}_h,\\
\eta_{E,\Gamma}^2&=h_E\|\boldsymbol{\lambda}_h+\boldsymbol{\sigma}(\boldsymbol{u}_h)\boldsymbol{n}\|_{0,E}^2, && E\in\mathcal{G}_h.
\end{aligned}
$$

Moreover, we define the additional terms at the contact boundary as

$$S^2=\|(g-u_{h,n})_-\|_{0,\Gamma}^2+((g-u_{h,n})_+,\lambda_{h,n})_\Gamma+\int_\Gamma(\kappa|\boldsymbol{u}_{h,t}|-\boldsymbol{u}_{h,t}\cdot\boldsymbol{\lambda}_{h,t})\,\mathrm{d}s.$$

Theorem 4 (a posteriori error estimate)**.**

$$\|(\boldsymbol{u}-\boldsymbol{u}_h,\boldsymbol{\lambda}-\boldsymbol{\lambda}_h)\|\lesssim\eta+S$$

Proof. In view of continuous stability there exists $\boldsymbol{v} \in \boldsymbol{V}$ such that

$$\begin{aligned}
&\|(\boldsymbol{u}-\boldsymbol{u}_h, \boldsymbol{\lambda}-\boldsymbol{\lambda}_h)\|^2 \\
&\lesssim \mathcal{B}(\boldsymbol{u}-\boldsymbol{u}_h, \boldsymbol{\lambda}-\boldsymbol{\lambda}_h; \boldsymbol{v}, \boldsymbol{\lambda}_h-\boldsymbol{\lambda}) \\
&= \mathcal{B}(\boldsymbol{u}, \boldsymbol{\lambda}, \boldsymbol{v}, \boldsymbol{\lambda}_h-\boldsymbol{\lambda}) - \mathcal{B}(\boldsymbol{u}_h, \boldsymbol{\lambda}_h; \boldsymbol{v}, \boldsymbol{\lambda}_h-\boldsymbol{\lambda}) \\
&\le \mathcal{L}(\boldsymbol{v}, \boldsymbol{\lambda}_h-\boldsymbol{\lambda}) - \mathcal{B}(\boldsymbol{u}_h, \boldsymbol{\lambda}_h; \boldsymbol{v}, \boldsymbol{\lambda}_h-\boldsymbol{\lambda}),
\end{aligned}$$

where in the last inequality we have used Problem 2. Let now $\widetilde{\boldsymbol{v}}$ be the Clément interpolant of $\boldsymbol{v}$. From the discrete problem (25), it follows that

$$0 \le -\mathcal{B}(\boldsymbol{u}_h, \boldsymbol{\lambda}_h; -\widetilde{\boldsymbol{v}}, \boldsymbol{0}) + \mathcal{L}(-\widetilde{\boldsymbol{v}}, \boldsymbol{0}) + \alpha \sum_{E\in\mathcal{G}_h} h_E(\boldsymbol{\lambda}_h + \boldsymbol{\sigma}(\boldsymbol{u}_h)\boldsymbol{n}, \boldsymbol{\sigma}(-\widetilde{\boldsymbol{v}})\boldsymbol{n})_E.$$

Using the above inequality and integration by parts, we get

$$\begin{aligned}
&\|(\boldsymbol{u}-\boldsymbol{u}_h, \boldsymbol{\lambda}-\boldsymbol{\lambda}_h)\|^2 \\
&\lesssim \mathcal{L}(\boldsymbol{v}-\widetilde{\boldsymbol{v}}, \boldsymbol{\lambda}_h-\boldsymbol{\lambda}) - \mathcal{B}(\boldsymbol{u}_h, \boldsymbol{\lambda}_h; \boldsymbol{v}-\widetilde{\boldsymbol{v}}, \boldsymbol{\lambda}_h-\boldsymbol{\lambda}) \\
&\quad + \alpha \sum_{E\in\mathcal{G}_h} h_E(\boldsymbol{\lambda}_h + \boldsymbol{\sigma}(\boldsymbol{u}_h)\boldsymbol{n}, \boldsymbol{\sigma}(-\widetilde{\boldsymbol{v}})\boldsymbol{n})_E \\
&= \sum_{K\in\mathcal{T}_h} (\operatorname{\mathbf{div}} \boldsymbol{\sigma}(\boldsymbol{u}_h) + \boldsymbol{f}, \boldsymbol{v}-\widetilde{\boldsymbol{v}})_K - \sum_{E\in\mathcal{E}_h} (\llbracket \boldsymbol{\sigma}(\boldsymbol{u}_h)\boldsymbol{n} \rrbracket, \boldsymbol{v}-\widetilde{\boldsymbol{v}})_E \\
&\quad - \sum_{E\in\mathcal{F}_h} (\boldsymbol{\sigma}(\boldsymbol{u}_h)\boldsymbol{n}, \boldsymbol{v}-\widetilde{\boldsymbol{v}})_E - \sum_{E\in\mathcal{G}_h} (\boldsymbol{\lambda}_h + \boldsymbol{\sigma}(\boldsymbol{u}_h)\boldsymbol{n}, \boldsymbol{v}-\widetilde{\boldsymbol{v}})_E \\
&\quad - b(\boldsymbol{u}_h, \boldsymbol{\lambda}_h-\boldsymbol{\lambda}) + \langle g, \lambda_{h,n}-\lambda_n\rangle + \alpha \sum_{E\in\mathcal{G}_h} h_E(\boldsymbol{\lambda}_h + \boldsymbol{\sigma}(\boldsymbol{u}_h)\boldsymbol{n}, \boldsymbol{\sigma}(-\widetilde{\boldsymbol{v}})\boldsymbol{n})_E.
\end{aligned}$$

The first four terms are bounded using the Cauchy–Schwarz inequality, continuous stability estimate, and the standard Clemént interpolation estimate:

$$\sum_{K\in\mathcal{T}_h} h_K^{-2}\|\boldsymbol{v}-\widetilde{\boldsymbol{v}}\|_{0,K}^2 + \sum_{E\in\mathcal{E}_h\cup\mathcal{F}_h\cup\mathcal{G}_h} h_E^{-1}\|\boldsymbol{v}-\widetilde{\boldsymbol{v}}\|_{0,E}^2 \lesssim |||\boldsymbol{v}|||^2.$$

The last term is estimated using the Cauchy–Schwarz inequality, Lemma 1, and the bound $|||\widetilde{\boldsymbol{v}}||| \lesssim |||\boldsymbol{v}|||$. The remaining terms are estimated as follows:

$$\begin{aligned}
&- b(\boldsymbol{u}_h, \boldsymbol{\lambda}_h-\boldsymbol{\lambda}) + \langle g, \lambda_{h,n}-\lambda_n\rangle \\
&= \langle g-u_{h,n}, \lambda_{h,n}-\lambda_n\rangle - \langle \boldsymbol{u}_{h,t}, \boldsymbol{\lambda}_{h,t}-\boldsymbol{\lambda}_t\rangle \\
&= \langle (g-u_{h,n})_-, \lambda_{h,n}-\lambda_n\rangle + \langle (g-u_{h,n})_+, \lambda_{h,n}-\lambda_n\rangle \\
&\quad - (\boldsymbol{u}_{h,t}, \boldsymbol{\lambda}_{h,t})_\Gamma + \langle \boldsymbol{u}_{h,t}, \boldsymbol{\lambda}_t\rangle \\
&\le \|(g-u_{h,n})_-\|_{1/2,\Gamma}\|\lambda_{h,n}-\lambda_n\|_{-1/2,\Gamma} + ((g-u_{h,n})_+, \lambda_{h,n})_\Gamma \\
&\quad + \int_\Gamma (\kappa|\boldsymbol{u}_{h,t}| - \boldsymbol{u}_{h,t}\cdot\boldsymbol{\lambda}_{h,t})\,\mathrm{d}s.
\end{aligned}$$

□

The proof of the following theorem is standard [24]; see also [9].

Theorem 5 (efficiency of the error indicator)**.**

$$\eta \lesssim \|(\boldsymbol{u}-\boldsymbol{u}_h, \boldsymbol{\lambda}-\boldsymbol{\lambda}_h)\| + \left(\sum_{E\in\mathcal{G}_h} \operatorname{osc}_{K(E)}(\boldsymbol{f})^2\right)^{1/2}.$$

6. Nitsche's method

Due to the stabilization terms, the Lagrange multiplier can be eliminated locally in each element. Choosing $\boldsymbol{v}_h = \boldsymbol{0}$ in the discrete problem gives

$$\begin{aligned}&(\boldsymbol{u}_h, \boldsymbol{\mu}_h - \boldsymbol{\lambda}_h)_\Gamma - \alpha \sum_{E\in\mathcal{G}_h} h_E(\boldsymbol{\lambda}_h + \boldsymbol{\sigma}(\boldsymbol{u}_h)\boldsymbol{n}, \boldsymbol{\mu}_h - \boldsymbol{\lambda}_h)_E \\ &\leq (g, \mu_{h,n} - \lambda_{h,n})_\Gamma \quad \forall \boldsymbol{\mu}_h \in \boldsymbol{\Lambda}_h.\end{aligned}$$

This inequality can be decomposed into normal and tangential parts by considering the test function $\boldsymbol{\mu}_h = \mu_{h,n}\boldsymbol{n} + \boldsymbol{\mu}_{h,t}$. Choosing first $\boldsymbol{\mu}_{h,t} = \boldsymbol{\lambda}_{h,t}$ and then $\mu_{h,n} = \lambda_{h,n}$ leads to the inequalities

$$(u_{h,n} - g, \mu_{h,n} - \lambda_{h,n})_\Gamma - \alpha \sum_{E\in\mathcal{G}_h} h_E(\lambda_{h,n} + \sigma_n(\boldsymbol{u}_h), \mu_{h,n} - \lambda_{h,n})_E \leq 0$$

and

$$(\boldsymbol{u}_{h,t}, \boldsymbol{\mu}_{h,t} - \boldsymbol{\lambda}_{h,t})_\Gamma - \alpha \sum_{E\in\mathcal{G}_h} h_E(\boldsymbol{\lambda}_{h,t} + \boldsymbol{\sigma}_t(\boldsymbol{u}_h)\boldsymbol{n}, \boldsymbol{\mu}_{h,t} - \boldsymbol{\lambda}_{h,t})_E \leq 0,$$

valid for every $(\mu_{h,n}, \boldsymbol{\mu}_{h,t}) \in \boldsymbol{\Lambda}_h$. Suppose now that $E \in \mathcal{G}_h$ is such that $|\boldsymbol{\lambda}_{h,t}(\boldsymbol{x})| < \kappa$ for any $\boldsymbol{x} \in E$. Then the test function

$$\boldsymbol{\mu}_{h,t}(\boldsymbol{x}) = \begin{cases} \boldsymbol{\lambda}_{h,t}(\boldsymbol{x}) \pm \varepsilon\boldsymbol{\varphi}_E(\boldsymbol{x}) & \text{if } \boldsymbol{x} \in E, \\ \boldsymbol{\lambda}_{h,t}(\boldsymbol{x}) & \text{otherwise,} \end{cases}$$

where $\boldsymbol{\varphi}_E$ is one of the basis functions of $\boldsymbol{Q}_h|_E$ and $\varepsilon > 0$ is sufficiently small so that $|\boldsymbol{\mu}_{h,t}| < \kappa$, gives

$$\begin{cases} (\boldsymbol{u}_{h,t} - \alpha h_E(\boldsymbol{\lambda}_{h,t} + \boldsymbol{\sigma}_t(\boldsymbol{u}_h)\boldsymbol{n}), \boldsymbol{\varphi}_E)_E \leq 0 \\ (\boldsymbol{u}_{h,t} - \alpha h_E(\boldsymbol{\lambda}_{h,t} + \boldsymbol{\sigma}_t(\boldsymbol{u}_h)\boldsymbol{n}), -\boldsymbol{\varphi}_E)_E \leq 0, \end{cases}$$

implying that

$$(\boldsymbol{u}_{h,t} - \alpha h_E(\boldsymbol{\lambda}_{h,t} + \boldsymbol{\sigma}_t(\boldsymbol{u}_h)\boldsymbol{n}), \boldsymbol{\varphi}_E)_E = 0.$$

Thus, we obtain the expression

$$\boldsymbol{\lambda}_{h,t} = \boldsymbol{\gamma}_t(\boldsymbol{u}_h) := \frac{1}{\alpha\mathcal{H}}\pi_h\boldsymbol{u}_{h,t} - \pi_h\boldsymbol{\sigma}_t(\boldsymbol{u}_h),$$

where π_h denotes the L^2-projection onto $\boldsymbol{Q}_h$ and $\mathcal{H} : \Gamma \to \mathbb{R}$, is such that $\mathcal{H}|_E = h_E$. Taking into account the entire boundary Γ and the case $|\boldsymbol{\lambda}_{h,t}| = \kappa$, the expression for the tangential Lagrange multiplier then reads as follows

$$\boldsymbol{\lambda}_{h,t} = \begin{cases} \boldsymbol{\gamma}_t(\boldsymbol{u}_h) & \text{if } |\boldsymbol{\gamma}_t(\boldsymbol{u}_h)| < \kappa, \\ \kappa\frac{\boldsymbol{\gamma}_t(\boldsymbol{u}_h)}{|\boldsymbol{\gamma}_t(\boldsymbol{u}_h)|} & \text{otherwise.} \end{cases} \tag{37}$$

Taking similar steps to eliminate the normal-directional Lagrange multiplier, we arrive at the expression

$$\lambda_{h,n} = \begin{cases} \gamma_n(\boldsymbol{u}_h) & \text{if } \gamma_n(\boldsymbol{u}_h) > 0, \\ 0 & \text{otherwise,} \end{cases} \tag{38}$$

where

$$\gamma_n(\boldsymbol{u}_h) := \frac{1}{\alpha\mathcal{H}}(\pi_h u_{h,n} - \pi_h g) - \pi_h\sigma_n(\boldsymbol{u}_h).$$

Testing with $\boldsymbol{v}_h$ in the discrete problem (25) and using expressions (37) and (38), leads to the variational equality

$$
\begin{aligned}
&(\boldsymbol{\sigma}(\boldsymbol{u}_h), \boldsymbol{\varepsilon}(\boldsymbol{v}_h))_\Omega \\
&+ b(\boldsymbol{v}_h, \boldsymbol{\lambda}_h) - \alpha \sum_{E \in \mathcal{G}_h} h_E(\boldsymbol{\lambda}_h + \boldsymbol{\sigma}(\boldsymbol{u}_h)\boldsymbol{n}, \boldsymbol{\sigma}(\boldsymbol{v}_h)\boldsymbol{n})_E \\
&= (\boldsymbol{f}, \boldsymbol{v}_h)_\Omega \quad \forall \boldsymbol{v}_h \in \boldsymbol{V}_h.
\end{aligned} \tag{39}
$$

Focusing on the terms

$$
b(\boldsymbol{v}_h, \boldsymbol{\lambda}_h) - \alpha \sum_{E \in \mathcal{G}_h} h_E(\boldsymbol{\lambda}_h + \boldsymbol{\sigma}(\boldsymbol{u}_h)\boldsymbol{n}, \boldsymbol{\sigma}(\boldsymbol{v}_h)\boldsymbol{n})_E, \tag{40}
$$

we first observe that the normal-directional part of (40) reads as follows

$$
(\lambda_{h,n}, v_{h,n})_\Gamma - \alpha \sum_{E \in \mathcal{G}_h} h_E(\lambda_{h,n} + \sigma_n(\boldsymbol{u}_h), \sigma_n(\boldsymbol{v}_h))_E.
$$

In view of (38) and the definition of $\gamma_n(\boldsymbol{u}_h)$, this can be written as

$$
\begin{aligned}
&\left(\tfrac{1}{\alpha\mathcal{H}} u_{h,n}, v_{h,n}\right)_{\Gamma_C} - (\alpha\mathcal{H}\sigma_n(\boldsymbol{u}_h), \sigma_n(\boldsymbol{v}_h))_{\Gamma\setminus\Gamma_C} \\
&- (\sigma_n(\boldsymbol{u}_h), v_{h,n})_{\Gamma_C} - (u_{h,n}, \sigma_n(\boldsymbol{v}_h))_{\Gamma_C} \\
&- \left(\tfrac{1}{\alpha\mathcal{H}} \pi_h g, v_{h,n}\right)_{\Gamma_C} + (\alpha\mathcal{H}\pi_h g, \sigma_n(\boldsymbol{v}_h))_{\Gamma_C}
\end{aligned} \tag{41}
$$

provided that $\boldsymbol{Q}_h$ has a large enough polynomial order ($l \geq m$) so that $\pi_h\sigma_n(\boldsymbol{u}_h) = \sigma_n(\boldsymbol{u}_h)$ and $\pi_h u_{h,n} = u_{h,n}$. Above, and in what follows,

$$
\Gamma_C = \Gamma_C(\boldsymbol{u}_h) = \{\boldsymbol{x} \in \Gamma : \gamma_n(\boldsymbol{u}_h(\boldsymbol{x})) > 0\}
$$

is defined as the active contact boundary.

The tangential part of (40) is

$$
(\boldsymbol{\lambda}_{h,t}, \boldsymbol{v}_{h,t})_\Gamma - \alpha \sum_{E \in \mathcal{G}_h} h_E(\boldsymbol{\lambda}_{h,t} + \boldsymbol{\sigma}_t(\boldsymbol{u}_h), \boldsymbol{\sigma}_t(\boldsymbol{v}_h))_E
$$

and, using (37), it can be expanded into

$$
\begin{aligned}
&\left(\tfrac{1}{\alpha\mathcal{H}} \boldsymbol{u}_{h,t}, \boldsymbol{v}_{h,t}\right)_{\Gamma_S} - (\alpha\mathcal{H}\boldsymbol{\sigma}_t(\boldsymbol{u}_h), \boldsymbol{\sigma}_t(\boldsymbol{v}_h))_{\Gamma\setminus\Gamma_S} \\
&- (\boldsymbol{\sigma}_t(\boldsymbol{u}_h), \boldsymbol{v}_{h,t})_{\Gamma_S} - (\boldsymbol{u}_{h,t}, \boldsymbol{\sigma}_t(\boldsymbol{v}_h))_{\Gamma_S} \\
&+ \left(\kappa \tfrac{\boldsymbol{\gamma}_t(\boldsymbol{u}_h)}{|\boldsymbol{\gamma}_t(\boldsymbol{u}_h)|}, \boldsymbol{v}_{h,t}\right)_{\Gamma\setminus\Gamma_S} - \left(\alpha\mathcal{H}\kappa \tfrac{\boldsymbol{\gamma}_t(\boldsymbol{u}_h)}{|\boldsymbol{\gamma}_t(\boldsymbol{u}_h)|}, \boldsymbol{\sigma}_t(\boldsymbol{v}_h)\right)_{\Gamma\setminus\Gamma_S}
\end{aligned} \tag{42}
$$

where we have defined $\Gamma_S = \Gamma_S(\boldsymbol{u}_h) = \{\boldsymbol{x} \in \Gamma : |\boldsymbol{\gamma}_t(\boldsymbol{u}_h(\boldsymbol{x}))| < \kappa\}$ as the part of Γ where the body sticks to the rigid foundation.

Combining (39), (41) and (42) leads to a Nitsche-type formulation of the discrete problem wherein the Lagrange multiplier is absent. Note that the new formulation is still nonlinear because the sets Γ_C and Γ_S depend on the solution $\boldsymbol{u}_h$ itself. Inspired by the primal-dual active set strategy proposed in [5], i.e. fixing the active sets Γ_C and Γ_S by repeatedly limiting the components of $\boldsymbol{\lambda}_h$ that violate the contact/friction conditions, we perform a fixed-point iteration where Γ_C and Γ_S are computed from the discrete solution of the previous iteration. The resulting method is summarized in Algorithm 1.

Algorithm 1 Contact iteration

Require: $\boldsymbol{V}_h$ is a finite element space
Require: $\epsilon > 0$ is a convergence tolerance

procedure NITSCHE($\boldsymbol{V}_h$, ϵ)
  $\boldsymbol{w}_h \leftarrow \boldsymbol{0}$
  repeat
    Find $\boldsymbol{u}_h \in \boldsymbol{V}_h$ such that

$$
\begin{aligned}
&(\boldsymbol{\sigma}(\boldsymbol{u}_h), \boldsymbol{\varepsilon}(\boldsymbol{v}_h))_\Omega \\
&+ \left(\tfrac{1}{\alpha\mathcal{H}} u_{h,n}, v_{h,n}\right)_{\Gamma_C(\boldsymbol{w}_h)} - (\alpha\mathcal{H}\sigma_n(\boldsymbol{u}_h), \sigma_n(\boldsymbol{v}_h))_{\Gamma\setminus\Gamma_C(\boldsymbol{w}_h)} \\
&- (\sigma_n(\boldsymbol{u}_h), v_{h,n})_{\Gamma_C(\boldsymbol{w}_h)} - (u_{h,n}, \sigma_n(\boldsymbol{v}_h))_{\Gamma_C(\boldsymbol{w}_h)} \\
&+ \left(\tfrac{1}{\alpha\mathcal{H}} \boldsymbol{u}_{h,t}, \boldsymbol{v}_{h,t}\right)_{\Gamma_S(\boldsymbol{w}_h)} - (\alpha\mathcal{H}\boldsymbol{\sigma}_t(\boldsymbol{u}_h), \boldsymbol{\sigma}_t(\boldsymbol{v}_h))_{\Gamma\setminus\Gamma_S(\boldsymbol{w}_h)} \\
&- (\boldsymbol{\sigma}_t(\boldsymbol{u}_h), \boldsymbol{v}_{h,t})_{\Gamma_S(\boldsymbol{w}_h)} - (\boldsymbol{u}_{h,t}, \boldsymbol{\sigma}_t(\boldsymbol{v}_h))_{\Gamma_S(\boldsymbol{w}_h)} \\
&= (\boldsymbol{f}, \boldsymbol{v}_h)_\Omega \\
&\quad - \left(\tfrac{1}{\alpha\mathcal{H}}\pi_h g, v_{h,n}\right)_{\Gamma_C(\boldsymbol{w}_h)} + (\alpha\mathcal{H}\pi_h g, \sigma_n(\boldsymbol{v}_h))_{\Gamma_C(\boldsymbol{w}_h)} \\
&\quad + \left(\kappa\tfrac{\boldsymbol{\gamma}_t(\boldsymbol{w}_h)}{|\boldsymbol{\gamma}_t(\boldsymbol{w}_h)|}, \boldsymbol{v}_{h,t}\right)_{\Gamma\setminus\Gamma_S(\boldsymbol{w}_h)} \\
&\quad - \left(\alpha\mathcal{H}\kappa\tfrac{\boldsymbol{\gamma}_t(\boldsymbol{w}_h)}{|\boldsymbol{\gamma}_t(\boldsymbol{w}_h)|}, \boldsymbol{\sigma}_t(\boldsymbol{v}_h)\right)_{\Gamma\setminus\Gamma_S(\boldsymbol{w}_h)} \qquad \forall \boldsymbol{v}_h \in \boldsymbol{V}_h
\end{aligned}
$$

    $\boldsymbol{w}_h \leftarrow \boldsymbol{u}_h$
  until $|||\boldsymbol{u}_h - \boldsymbol{w}_h||| < \epsilon$
  return $\boldsymbol{u}_h$
end procedure

Remark 4. There are several possibilities for doing the comparisons $\gamma_n(\boldsymbol{u}_h) > 0$ and $|\boldsymbol{\gamma}_t(\boldsymbol{u}_h)| < \kappa$ in a practical implementation of Algorithm 1. For example, the sign of $\gamma_n(\boldsymbol{u}_h)$ may change inside an element and, therefore, an exact integration is unfeasible unless the active contact boundary Γ_C is known a priori. Some options include defining the active contact boundary element-by-element while looking at the mean value of $\gamma_n(\boldsymbol{u}_h)$, or performing the comparison $\gamma_n(\boldsymbol{u}_h) > 0$ separately at each quadrature point. See the source code of the numerical example [12] for more details on our implementation of Algorithm 1.

Remark 5. The stabilized method of Problem 3 can be implemented directly via a primal-dual active set strategy as demonstrated in [9] for the closely related obstacle problem. Such an approach is straightforward to realize using a piecewise-constant or discontinuous piecewise-linear Lagrange multiplier and may be computationally less intensive than Algorithm 1 since it avoids the reassembly of the terms (41) and (42) during each iteration.

7. Numerical experiment

Let us consider the domain $\Omega = (-0.5, 0.5)^2$ with $x = 0.5$, $x = -0.5$ and $y = \pm 0.5$ corresponding to Γ, Γ_D and Γ_N, respectively. We set $\boldsymbol{f} = \boldsymbol{0}$, $g = -0.1$, $E = 1$, $\nu = 0.3$, and $\kappa = 0.2$. The numerical experiment is implemented using scikit-fem [25] which relies heavily on the SciPy ecosystem [26]. The figures are

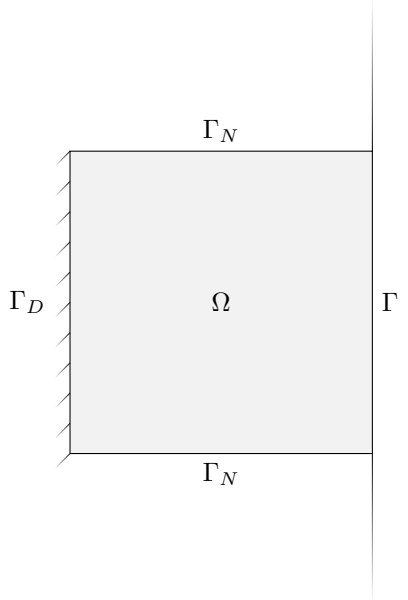

FIGURE 1. Problem setting for the numerical example. The rigid foundation (on the right) moves 0.1 units to the left.

created with the help of matplotlib [27] and the full source code of the experiment is available in [12].

Using quadratic finite elements, a uniform mesh with $h \approx 0.044$ and $\alpha = 10^{-3}$ for Algorithm 1, we obtain the Lagrange multipliers depicted in Figure 2. The value of the stabilization parameter α has been chosen by trial-and-error so that the resulting linear system is well conditioned—see Theorem 2. The absolute value of the tangential multiplier is limited by the bound $\kappa = 0.2$, as expected, and the normal multiplier remains positive on the entire contact boundary. In the absence of an analytical solution, we evaluate the vectorial H^1-norm of the discrete displacement and the total error estimator η and the term S for a sequence of uniform meshes; see Table 1 with the required number of contact iterations depicted in Figure 6.

In an attempt to improve over the uniform meshing strategy, we solve the same problem using adaptive mesh refinement and terminate the refinement loop after the number of degrees-of-freedom N is above a given threshold. We use Nitsche's method as given in Algorithm 1 and calculate the error estimators (36) with Lagrange multipliers given by the formulae (37) and (38). The results, computed using the final adaptive mesh, are given in Figure 3. Visually, the improvement in the Lagrange multipliers is obvious although N is roughly the same as in Figure 2. In addition, comparing the values of $\|\boldsymbol{u}_h\|_1$ in Tables 1 and 2 reveals that the vectorial H^1-norm of the solution is close to what would be expected from the uniform mesh with 132,098 degrees-of-freedom.

A careful comparison of the values of η in Tables 1 and 2 shows that the adaptive meshing appears to improve the convergence rate asymptotically to $O(N^{-1})$ which is the expected rate of convergence for a smooth solution and quadratic elements;

see also Figure 4 for a visualization of the total error estimator η, Figure 5 for a visualization of the different components of η and the term S, and Figure 6 for the required number of contact iterations. Thus, we conclude that while the convergence rate of the uniform strategy is limited by the regularity of the exact solution, the adaptive strategy successfully regains the optimal convergence rate with respect to the number of degrees-of-freedom.

TABLE 1. The norm of the solution and the value of the total error indicator η and the term S using a uniform mesh family. The number of degrees-of-freedom is denoted by N.

h	N	$\|\boldsymbol{u}_h\|_1$	η	S
0.35	162	0.125125	$2.43 \cdot 10^{-2}$	$9.86 \cdot 10^{-5}$
0.18	578	0.125212	$1.43 \cdot 10^{-2}$	$3.88 \cdot 10^{-5}$
$8.84 \cdot 10^{-2}$	2,178	0.125337	$8.51 \cdot 10^{-3}$	$1.88 \cdot 10^{-5}$
$4.42 \cdot 10^{-2}$	8,450	0.125362	$5.06 \cdot 10^{-3}$	$3.95 \cdot 10^{-6}$
$2.21 \cdot 10^{-2}$	33,282	0.125377	$3.03 \cdot 10^{-3}$	$2.46 \cdot 10^{-6}$
$1.10 \cdot 10^{-2}$	132,098	0.125382	$1.83 \cdot 10^{-3}$	$9.83 \cdot 10^{-7}$

TABLE 2. The norm of the solution and the value of the total error indicator η and the term S using an adaptive mesh family. The number of degrees-of-freedom is denoted by N.

N	$\|\boldsymbol{u}_h\|_1$	η	S
162	0.125125	$2.43 \cdot 10^{-2}$	$9.86 \cdot 10^{-5}$
222	0.12527	$2.00 \cdot 10^{-2}$	$9.84 \cdot 10^{-5}$
354	0.125444	$1.27 \cdot 10^{-2}$	$9.19 \cdot 10^{-5}$
426	0.125474	$1.09 \cdot 10^{-2}$	$9.18 \cdot 10^{-5}$
618	0.125482	$8.22 \cdot 10^{-3}$	$8.08 \cdot 10^{-5}$
910	0.125373	$5.62 \cdot 10^{-3}$	$3.92 \cdot 10^{-5}$
1,288	0.125385	$3.80 \cdot 10^{-3}$	$3.18 \cdot 10^{-5}$
1,430	0.12539	$3.34 \cdot 10^{-3}$	$2.05 \cdot 10^{-5}$
1,534	0.125391	$3.20 \cdot 10^{-3}$	$2.05 \cdot 10^{-5}$
1,962	0.125394	$2.48 \cdot 10^{-3}$	$2.05 \cdot 10^{-5}$
2,210	0.125383	$2.24 \cdot 10^{-3}$	$6.91 \cdot 10^{-6}$
2,718	0.125384	$1.82 \cdot 10^{-3}$	$6.90 \cdot 10^{-6}$
2,946	0.125384	$1.62 \cdot 10^{-3}$	$6.99 \cdot 10^{-6}$
3,354	0.125385	$1.36 \cdot 10^{-3}$	$6.99 \cdot 10^{-6}$
3,766	0.125385	$1.23 \cdot 10^{-3}$	$6.99 \cdot 10^{-6}$
4,270	0.125385	$1.09 \cdot 10^{-3}$	$5.46 \cdot 10^{-6}$
5,184	0.125386	$9.10 \cdot 10^{-4}$	$5.22 \cdot 10^{-6}$
5,800	0.125386	$8.10 \cdot 10^{-4}$	$5.17 \cdot 10^{-6}$
6,376	0.125386	$7.42 \cdot 10^{-4}$	$5.17 \cdot 10^{-6}$
6,640	0.125386	$7.09 \cdot 10^{-4}$	$5.17 \cdot 10^{-6}$
7,946	0.125386	$6.03 \cdot 10^{-4}$	$3.04 \cdot 10^{-6}$

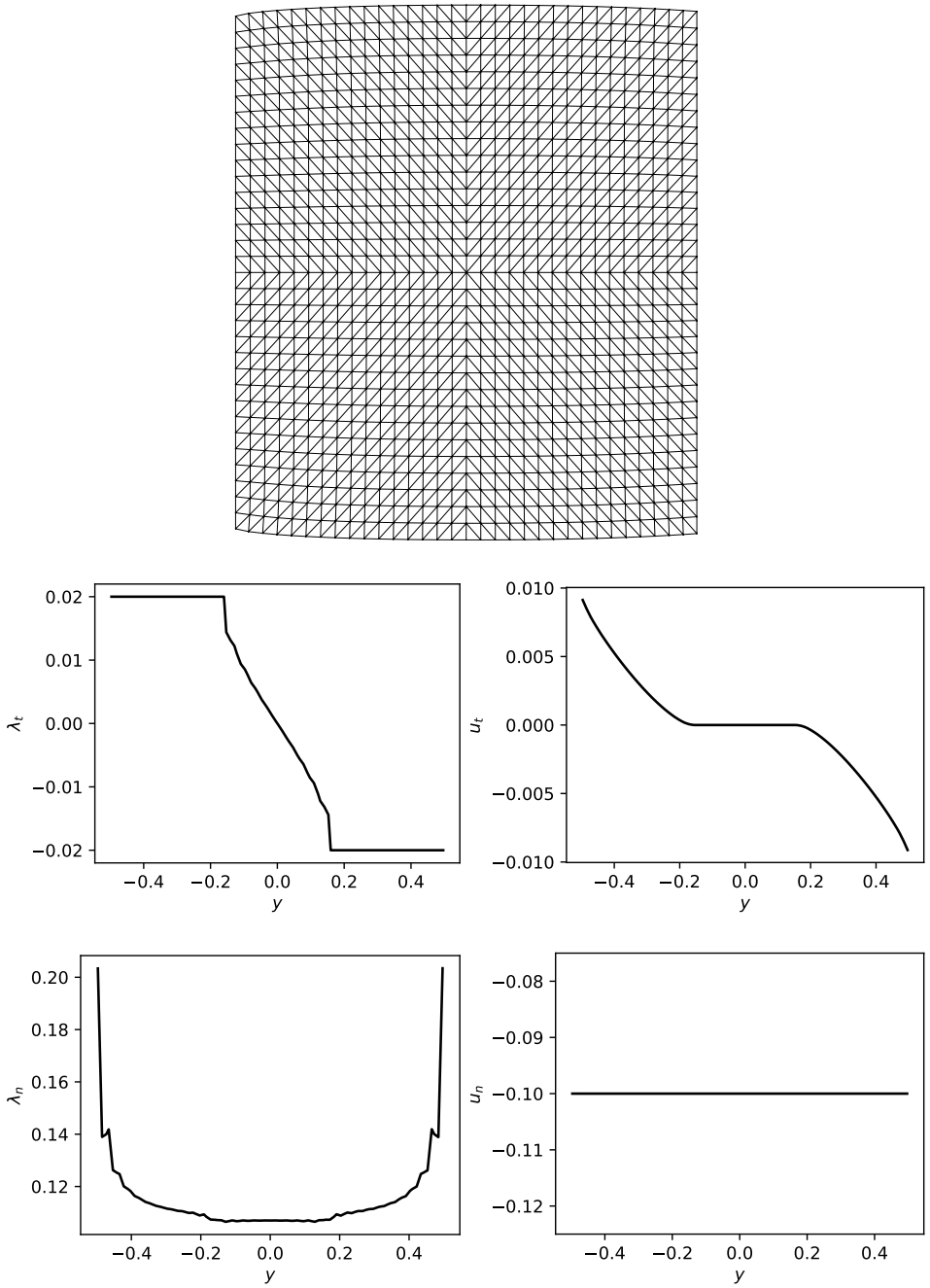

FIGURE 2. From top to bottom: the deformed, uniformly refined mesh with the number of degrees-of-freedom $N = 8{,}450$, the tangential and the normal Lagrange multiplier as a function of y.

ACKNOWLEDGEMENTS

This work was supported by the Academy of Finland (Decisions 324611 and 338341) and by the Portuguese government through FCT (Fundação para a Ciência

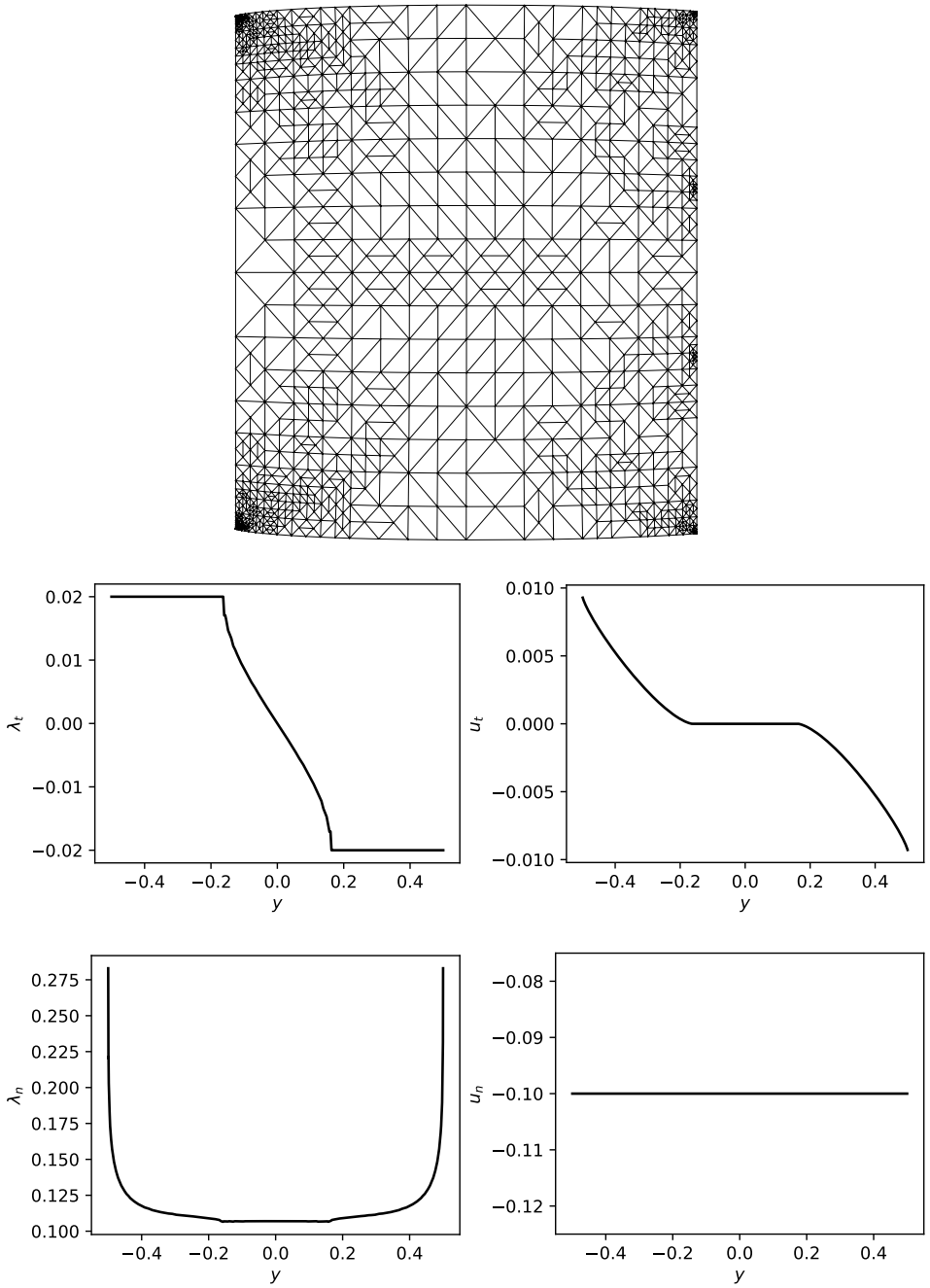

FIGURE 3. From top to bottom: the deformed, adaptively refined mesh with the number of degrees-of-freedom $N = 7{,}946$, the tangential and the normal Lagrange multiplier as a function of y.

e a Tecnologia), I.P., under the projects PTDC/MAT-PUR/28686/2017 and UIDB/04459/2020.

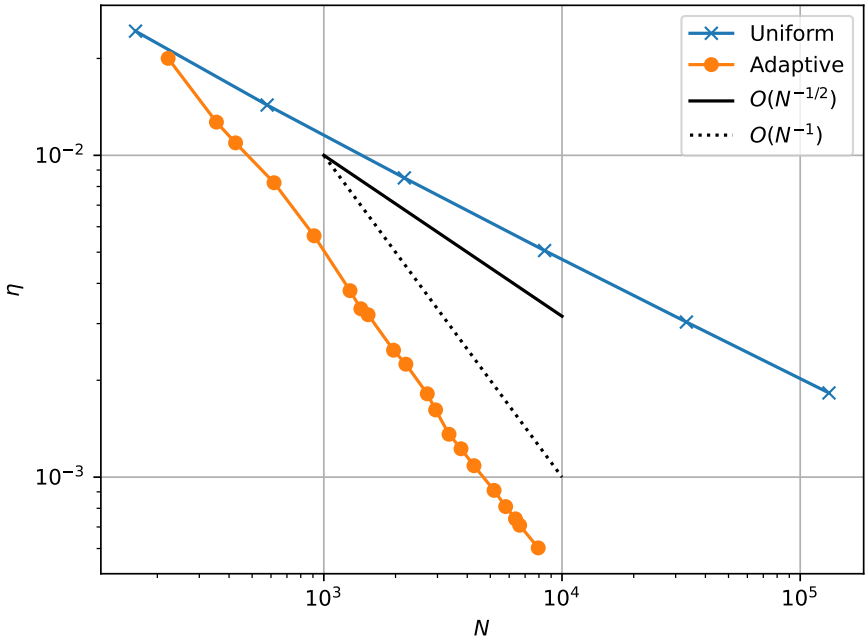

FIGURE 4. The total error indicator η as a function of the number of degrees-of-freedom N.

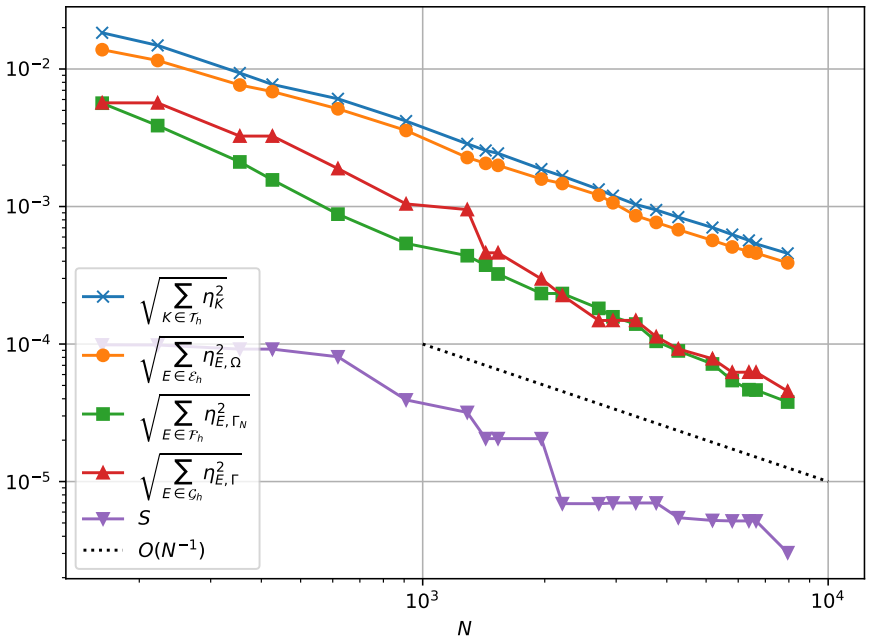

FIGURE 5. The different components of the total error estimator as a function of the number of degrees-of-freedom N for the adaptive mesh family.

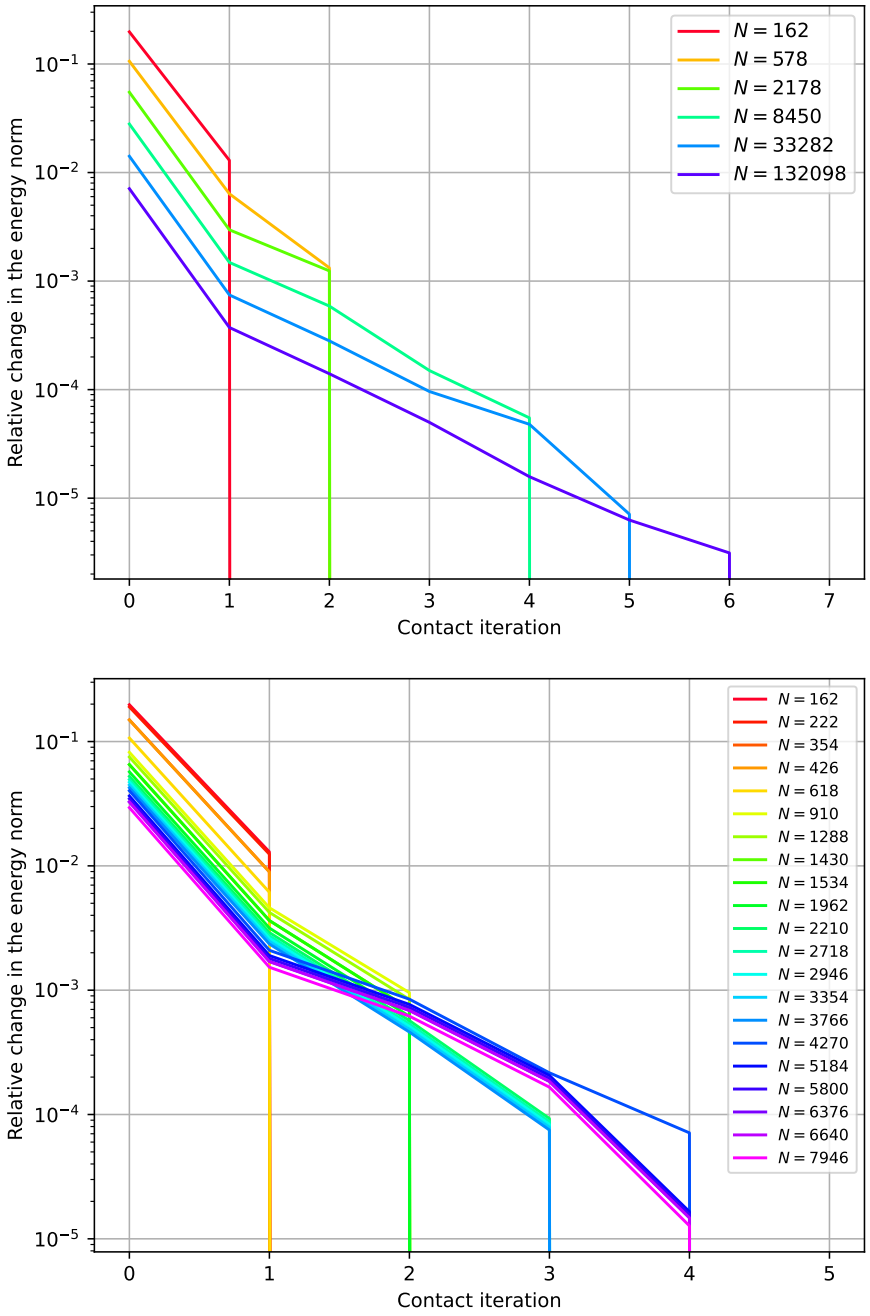

FIGURE 6. A visualization of the number of contact iterations required before the energy norm error between two consecutive approximations reaches machine epsilon for the uniformly (top) and the adaptively (bottom) refined meshes. The downwards pointing line signifies that the active contact set has converged.

References

[1] N. Kikuchi, J. T. Oden, Contact Problems in Elasticity: A Study of Variational Inequalities and Finite Element Methods, SIAM, Philadelphia, 1988. doi:10.1137/1.9781611970845.

[2] J. Haslinger, I. Hlaváček, J. Nečas, Numerical methods for unilateral problems in solid mechanics, in: Finite Element Methods (Part 2), Numerical Methods for Solids (Part 2), Vol. 4 of Handbook of Numerical Analysis, Elsevier, 1996, pp. 313–485. doi:10.1016/S1570-8659(96)80005-6.

[3] P. Wriggers, Computational Contact Mechanics, 2nd Ed., Springer-Verlag, Berlin Heidelberg, 2006. doi:10.1007/978-3-540-32609-0.

[4] G. Duvaut, J. L. Lions, Inequalities in Mechanics and Physics, Springer, Berlin, 1976. doi:10.1007/978-3-642-66165-5.

[5] B. Wohlmuth, Variationally consistent discretization schemes and numerical algorithms for contact problems, Acta Numerica 20 (2011) 569–734. doi:10.1017/S0962492911000079.

[6] F. Chouly, An adaptation of Nitsche's method to the Tresca friction problem, Journal of Mathematical Analysis and Applications 411 (1) (2014) 329–339. doi:10.1016/j.jmaa.2013.09.019.

[7] F. Chouly, R. Mlika, Y. Renard, An unbiased Nitsche's approximation of the frictional contact between two elastic structures, Numerische Mathematik 139 (3) (2018) 593–631. doi:10.1007/s00211-018-0950-x.

[8] F. Chouly, M. Fabre, P. Hild, J. Pousin, Y. Renard, Residual-based a posteriori error estimation for contact problems approximated by Nitsche's method, IMA Journal of Numerical Analysis 38 (2) (2018) 921–954. doi:10.1093/imanum/drx024.

[9] T. Gustafsson, R. Stenberg, J. Videman, Mixed and stabilized finite element methods for the obstacle problem, SIAM Journal on Numerical Analysis 55 (6) (2017) 2718–2744. doi:10.1137/16M1065422.

[10] T. Gustafsson, R. Stenberg, J. Videman, On Nitsche's method for elastic contact problems, SIAM Journal on Scientific Computing 42 (2) (2020) B425–B446. doi:10.1137/19M1246869.

[11] P. Hild, Y. Renard, A stabilized Lagrange multiplier method for the finite element approximation of contact problems in elastostatics, Numerische Mathematik 115 (1) (2010) 101–129. doi:10.1007/s00211-009-0273-z.

[12] T. Gustafsson, Source code for the numerical experiment: kinnala/paper-fricnitsche (2022). doi:10.5281/zenodo.5851711.

[13] T. A. Laursen, Computational Contact and Impact Mechanics, corr. 2nd printing, Springer, Heidelberg, 2003. doi:10.1007/978-3-662-04864-1.

[14] J. Haslinger, I. Hlaváçek, Approximation of the Signorini problem with friction by a mixed finite element method, Journal of Mathematical Analysis and Applications 86 (1) (1982) 99–122. doi:10.1016/0022-247X(82)90257-8.

[15] L. Baillet, T. Sassi, Mixed finite element methods for the Signorini problem with friction, Numerical Methods for Partial Differential Equations 22 (6) (2006) 1489–1508. doi:10.1002/num.20147.

[16] J. Haslinger, T. Sassi, Mixed finite element approximation of 3D contact problems with given friction: Error analysis and numerical realization, ESAIM: Mathematical Modelling and Numerical Analysis 38 (3) (2004) 563–578. doi:10.1051/m2an:2004026.

[17] P. Hild, Y. Renard, An error estimate for the Signorini problem with Coulomb friction approximated by finite elements, SIAM Journal on Numerical Analysis 45 (5) (2007) 2012–2031. doi:10.1137/050645439.

[18] S. Hüeber, G. Stadler, B. I. Wohlmuth, A primal-dual active set algorithm for three-dimensional contact problems with Coulomb friction, SIAM Journal on Scientific Computing 30 (2) (2008) 572–596. doi:10.1137/060671061.

[19] F. Chouly, A. Ern, N. Pignet, A hybrid high-order discretization combined with Nitsche's method for contact and Tresca friction in small strain elasticity, SIAM Journal on Scientific Computing 42 (4) (2020) A2300–A2324. doi:10.1137/19M1286499.

[20] P. Hild, V. Lleras, Residual error estimators for Coulomb friction, SIAM Journal on Numerical Analysis 47 (5) (2009) 3550–3583. doi:10.1137/070711554.

[21] P. Dörsek, J. Melenk, Adaptive hp-FEM for the contact problem with Tresca friction in linear elasticity: The primal-dual formulation and a posteriori error estimation, Applied Numerical Mathematics 60 (7) (2010) 689–704. doi:10.1016/j.apnum.2010.03.011.

[22] P. Laborde, Y. Renard, Fixed point strategies for elastostatic frictional contact problems, Mathematical Methods in the Applied Sciences 31 (4) (2008) 415–441. doi:10.1002/mma.921.
[23] F. Chouly, M. Fabre, P. Hild, R. Mlika, J. Pousin, Y. Renard, An overview of recent results on Nitsche's method for contact problems, in: S. Bordas, E. Burman, M. Larson, M. Olshanskii (Eds.), Geometrically Unfitted Finite Element Methods and Applications, Vol. 121 of Lecture Notes in Computational Science and Engineering, Springer, 2017. doi:10.1007/978-3-319-71431-8_4.
[24] R. Verfürth, A Posteriori Error Estimation Techniques for Finite Element Methods, Oxford University Press, Oxford, 2013. doi:10.1093/acprof:oso/9780199679423.001.0001.
[25] T. Gustafsson, G. D. McBain, scikit-fem: A Python package for finite element assembly, Journal of Open Source Software 5 (52) (2020) 2369. doi:10.21105/joss.02369.
[26] P. Virtanen, R. Gommers, T. E. Oliphant, M. Haberland, T. Reddy, D. Cournapeau, E. Burovski, P. Peterson, W. Weckesser, J. Bright, S. J. van der Walt, M. Brett, J. Wilson, K. Jarrod Millman, N. Mayorov, A. R. J. Nelson, E. Jones, R. Kern, E. Larson, C. Carey, İ. Polat, Y. Feng, E. W. Moore, J. VanderPlas, D. Laxalde, J. Perktold, R. Cimrman, I. Henriksen, E. A. Quintero, C. R. Harris, A. M. Archibald, A. H. Ribeiro, F. Pedregosa, P. van Mulbregt, SciPy 1.0 Contributors, SciPy 1.0: Fundamental algorithms for scientific computing in Python, Nature Methods 17 (2020) 261–272. doi:10.1038/s41592-019-0686-2.
[27] J. D. Hunter, Matplotlib: A 2d graphics environment, Computing in Science & Engineering 9 (3) (2007) 90–95. doi:10.1109/MCSE.2007.55.

(Tom Gustafsson) Aalto University, Department of Mathematics and Systems Analysis, P.O. Box 11100 FI-00076 Aalto, Finland

(Juha Videman) CAMGSD and Mathematics Department, Instituto Superior Técnico, Universidade de Lisboa, Av. Rovisco Pais 1, 1049-001 Lisboa, Portugal